Applied Surface Science 276 (2013) 731–743

Contents lists available at SciVerse ScienceDirect

Applied Surface Science

journal homepage: www.elsevier.com/locate/apsusc

Experimental investigation on material migration phenomena in micro-EDM of reaction-bonded silicon carbide

Pay Jun Liew[a,c], Jiwang Yan[b,*], Tsunemoto Kuriyagawa[a]

[a] Department of Mechanical Systems and Design, Tohoku University, Aramaki Aoba 6-6-01, Aoba-ku, Sendai, 980-8579, Japan
[b] Department of Mechanical Engineering, Faculty of Science and Technology, Keio University, Hiyoshi 3-14-1, Kohoku-ku, Yokohama, 223-8522, Japan
[c] Manufacturing Process Department, Faculty of Manufacturing Engineering, Universiti Teknikal Malaysia Melaka, Hang Tuah Jaya, 76100, Durian Tunggal, Melaka, Malaysia

ARTICLE INFO

Article history:
Received 15 December 2012
Received in revised form 23 March 2013
Accepted 25 March 2013
Available online 2 April 2013

Keywords:
Micro electro discharge machining
Material migration
Material deposition
Carbon nanofibre
Reaction-bonded silicon carbide
Tungsten particle

ABSTRACT

Material migration between tool electrode and workpiece material in micro electrical discharge machining of reaction-bonded silicon carbide was experimentally investigated. The microstructural changes of workpiece and tungsten tool electrode were examined using scanning electron microscopy, cross sectional transmission electron microscopy and energy dispersive X-ray under various voltage, capacitance and carbon nanofibre concentration in the dielectric fluid. Results show that tungsten is deposited intensively inside the discharge-induced craters on the RB-SiC surface as amorphous structure forming micro particles, and on flat surface region as a thin interdiffusion layer of poly-crystalline structure. Deposition of carbon element on tool electrode was detected, indicating possible material migration to the tool electrode from workpiece material, carbon nanofibres and dielectric oil. Material deposition rate was found to be strongly affected by workpiece surface roughness, voltage and capacitance of the electrical discharge circuit. Carbon nanofibre addition in the dielectric at a suitable concentration significantly reduced the material deposition rate.

1. Introduction

In recent years, the use of ceramics in mechanical and manufacturing engineering has received intensive attention, due to their outstanding material properties. However, because of their high hardness, ceramics are difficult to be formed to complex geometries by traditional machining processes [1]. Recently, the use of electrical discharge machining (EDM) to machine ceramics has become a new research focus, owing to its advantages such as low installation cost and ability to machine complex three-dimensional shapes easily regardless of material hardness [2].

Many previous studies have been conducted to improve the machining efficiency and accuracy of ceramics by using EDM, and great progress has been made in this area. Pioneer work can be traced to Mohri et al. [3], who reported that the machining of insulating ceramics can be realized in EDM by assisting electrode method. Liu et al. [4] employed a steel toothed wheel as the tool electrode to machine high resistivity SiC ceramics using electrical discharge milling. The feasibility of EDM for machining non-conductive ceramics ZrO_2 and Al_2O_3 using adherent copper foil was conducted by Lin et al. [5]. Fukuzawa et al. [6] and Clijsters et al. [7] fabricated three-dimensional complex shape successfully on ceramics by EDM. A comparative study of the die-sinking EDM of three different ceramic materials has been carried out by Puertas and Luis [8].

However, a few problems still exist which limit the application of EDM technology to high value-added manufacturing industries. For example, the EDM fabricated surface is quite rough due to the electrical discharge induced craters. The melting and resolidification of material causes surface property change of the workpiece material. Another problem is that during electrical discharges, material migrations occur from the electrode to the workpiece [9]. The material migration leads to deposition of tool material to the workpiece surface, causing surface contamination. Especially when performing EDM in the micro/nano scale, the effect of material migration may play an important role from viewpoint of mechanical and physical properties of the machined surface.

The material migration phenomenon in EDM has been studied by many previous researchers. For instance, electro erosion of various metal materials, such as A1, Cr, Cu, Fe, and Zn, has been investigated by Greene and Guerrero-Alvarez [10]. Jeswani and Basu [11] studied the deposition and diffusion of copper and brass tool materials on mild steel, high carbon steel and high speed steel. Soni and Chakraverti [12] reported the change in chemical composition due to the migration of copper–tungsten tool material to workpiece during EDM of die steel. The material migration

* Corresponding author. Tel.: +81 455661445; fax: +81 455661495.
E-mail address: yan@mech.keio.ac.jp (J. Yan).

0169-4332/$ – see front matter © 2013 Elsevier B.V. All rights reserved.
http://dx.doi.org/10.1016/j.apsusc.2013.03.161

phenomena in EDM using suspended powder [13,14], powder compact and multi-layer electrodes [15–17] and combination of powder and powder metallurgy electrode [18] have also been investigated. Murray et al. [19] reported reverse-direction material migration, i.e., the attachment of workpiece debris on the tool electrodes. Apart from the material transfer between the tool and workpiece, Mafarona [20] and Jahan et al. [21] found that an amount of carbon migrates to both tool electrode and workpiece due to the decomposition of dielectric fluid. Kruth et al. [22], Ekmekci [23] and Thomson [24] showed that the carbon in the white layer on machined surface mainly comes from the hydrocarbon based dielectric fluid. However, most of the previous works have focused on material migration in EDM of high conductivity materials, whereas there is no available literature on that of low-conductivity ceramic materials.

In a recent paper of the present authors [25], we carried out micro EDM experiments on reaction-bonded silicon carbide (RB-SiC), an important ceramic material which has extremely low electrical conductivity. We found that by adding carbon nanofibres in the dielectric fluid, the EDM characteristics were significantly improved in terms of material removal rate, machined surface quality and tool electrode wear. This technology provides possibility for high-efficiency precision manufacturing of micro structures on ultra-hard ceramic materials. However, the material migration in micro EDM of RB-SiC and its effects on the machining process is still unknown. Therefore, in this work, we aimed to investigate the material migration phenomenon during the micro EDM of RB-SiC and to clarify its fundamental mechanism. The final objective is to find optimal conditions to control the material migration in micro EDM of ceramic materials and to improve the finished surface topography and surface integrity.

2. Experimental methods

2.1. Equipment and materials

The experiments were carried out using a micro EDM machine Panasonic MG-ED82W. This machine has a Resistor–Capacitor (RC) discharge circuit, with a stepping resolution of 0.1 μm. Fig. 1 shows a schematic diagram of the experimental setup.

RB-SiC ceramic with electrical resistivity (~1453 Ωcm) produced by Japan Fine Ceramics Co., Ltd. was selected as workpiece material. The RB-SiC material composed of 6H-SiC grains (average size <1 μm) and a Si matrix (approximately 10% in volume). Before EDM experiments, the surface microstructures of the RB-SiC ceramic were examined using transmission electron microscopy (TEM), as presented in Fig. 2. In the TEM micrograph, dark grey grains are 6H-SiC and the light grey regions around them are intergrain Si bonds (size less than 1 μm). It is noticed that a few 6H-SiC grains are directly bonded to each other without the presence of Si bonds at the grain boundaries, resulting in a very dense structure.

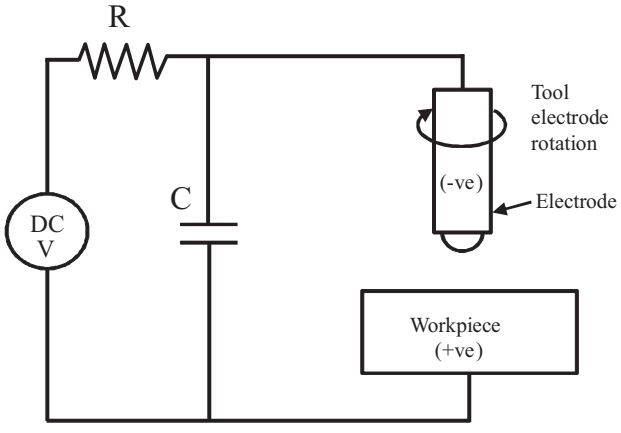

Fig. 1. Schematic diagram of the EDM experimental setup.

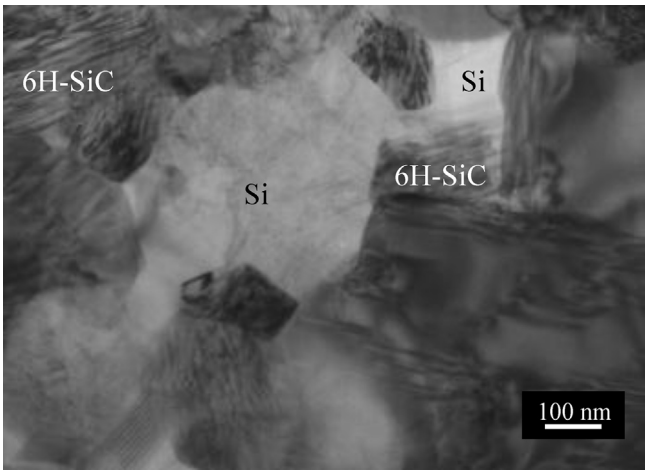

Fig. 2. Microstructures of RB-SiC observed by TEM.

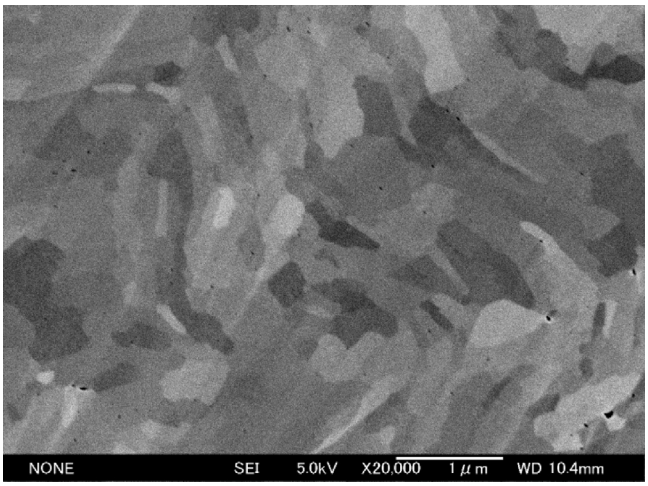

Fig. 3. SEM micrograph of tungsten grain.

Tungsten rods with 300 μm diameters were used as tool electrodes. A cross section sample of a tungsten electrode was prepared using ion milling and was observed using SEM, as shown in Fig. 3. It shows that most of the grains of tungsten are long and thin, the average size of which is about 1 μm. The electrodes were formed into hemi-spherical shapes with 100 μm radii by the wire electrical discharge grinding (WEDG) unit equipped in the experimental setup. Some typical material properties of the workpiece and the electrode are listed in Tables 1 and 2, respectively.

Table 1
Materials properties of RB-SiC (workpiece) [26].

Properties	Values
Grain size (μm)	<1
Volume (%)	Si-12, 6H-SiC-88
Density ρ (g/cm^3)	3.12
Softening temperature (°C)	1375
Electrical resistivity (Ω cm)	~1453
Young modulus E (GPa)	407
Vickers hardness (GPa)	25–35
Thermal conductivity (W/m K)	143

Table 2
Materials properties of tungsten (electrode) [27].

Properties	Values
Grain size (μm)	~1
Volume (%)	99.9
Density ρ (g/cm^3)	19.3
Melting temperature (°C)	3380
Electrical resistivity (Ω cm)	5.65×10^{-6}
Young modulus E (GPa)	411
Vickers hardness (MPa)	3430
Thermal conductivity (W/m K)	173

2.2. EDM conditions

Each micro EDM test was performed on the sample for duration of 3 min, and average of three tests for each parameter setting was taken. EDM oil CASTY-LUBE EDS was used as dielectric fluid first, and then carbon nanofibres were added into the EDM oil at different concentrations for comparison. The voltage and capacitance of the electrical discharge circuit were changed, and the extent of material migrations between the tool electrode and the RB-SiC workpiece was investigated experimentally. The experimental conditions are summarized in Table 3.

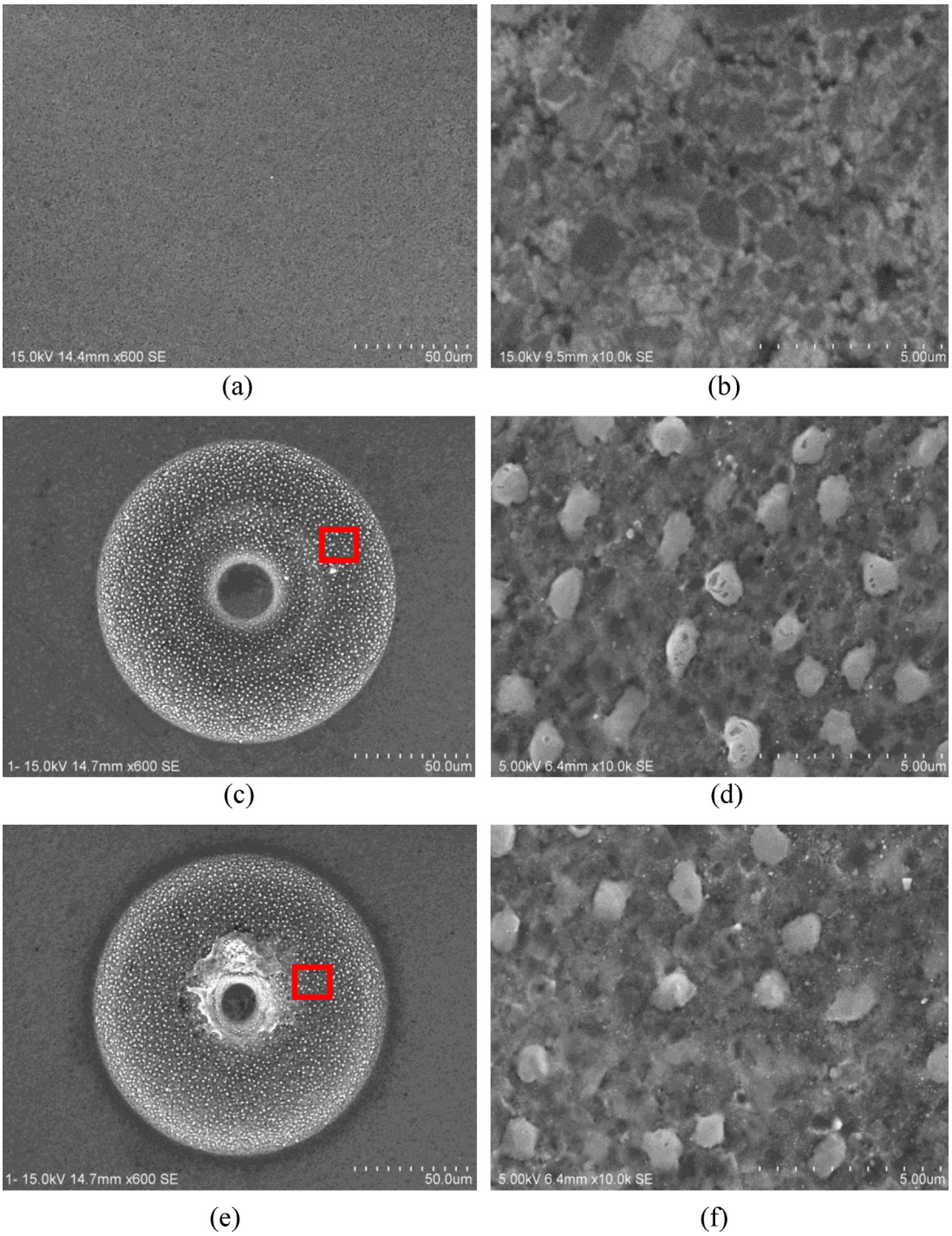

Fig. 4. SEM micrographs of (a) unmachined surface, (b) unmachined surface at high magnification, (c) micro cavity machined without carbon nanofibres, (d) tungsten deposition in a rectangle (c), (e) micro cavity machined with 0.06 g/L carbon nanofibres, (f) tungsten deposition in a rectangle (e).

Table 3
Experimental conditions.

Workpiece material	RB-SiC
Electrode material	Tungsten
Polarity	Positive (workpiece) Negative (tool)
Rotational speed (rpm)	3000
Feed rate (μm/s)	3
Voltage (V)	60–110
Condenser capacitance (pF)	stray capacitance (~1), 10, 110, 220, 3300
Dielectric fluid	EDM oil CASTY-LUBE EDS
Additive	Carbon nanofibre (CNF)
CNF size (μm)	diameter = 0.15, length = 6–8
Concentration (g/L)	0.06–0.28
Machining time (min)	3

2.3. Characterization

In order to examine the microstructure of the samples, surface topography of the machined micro cavity was examined using SEM. Subsequently, energy dispersive X-ray (EDX) was used to detect material migration and measure the amount of migrated material. Talymap software developed by Taylor Hobson Ltd., UK [28], was used to process the SEM photograph to quantify the size of migrated particles. In order to clarify the microstructures of migrated material, the cross sections of machined micro cavities and tool electrode tips were observed using TEM. Mechanical polishing and focused ion beam (FIB) techniques were used to prepare the TEM samples.

3. Results and discussion

3.1. Material deposition phenomena

In the experiments, we found that the finished surface of RB-SiC is covered by small particles after EDM under a few conditions. For example, Fig. 4(c) and (e) shows SEM micrographs of micro cavities obtained under fine machining conditions (voltage 80 V, stray capacitance ~1 pF) with/without adding carbon nanofibres in dielectric oil, respectively. In the figure, (d) and (f) are high-magnification views of the micro cavities in (c) and (e), respectively. It can be seen that for both machining conditions, lots of small white particles (size ~1 μm) have been formed on the machined surface, which are uniform in size and distribution. Since these white particles did not appear before the EDM tests, as depicted in Fig. 4(a) and (b), we can say that the particles have been generated during EDM due to material migration and deposition on the machined surface. In Fig. 4(c) and (e), cone shape protrusions are seen at the centre of the micro cavities, which were caused by the decentring of the tool electrodes.

In order to confirm the elemental composition of the white particles, the machined surface was analyzed using EDX at two different locations, particle region A and particle-free region B, as indicated in Fig. 5(a). As shown in Fig. 5(b), the EDX spectrum for Zone A consists of tungsten (W) at high weight percentage (89.96%). This result demonstrates that the white particles on the machined surface are mainly tungsten, which has been migrated from the tool electrode and deposited on the machined surface during the micro EDM process. In Zone B, tungsten was also detected but the weight percentage is low (25.58%), as depicted in Fig. 5(c). The silicon (Si) element in the spectra should be from the parent material RB-SiC, and the carbon (C) element might be from the parent material RB-SiC and/or the CNFs in the dielectric.

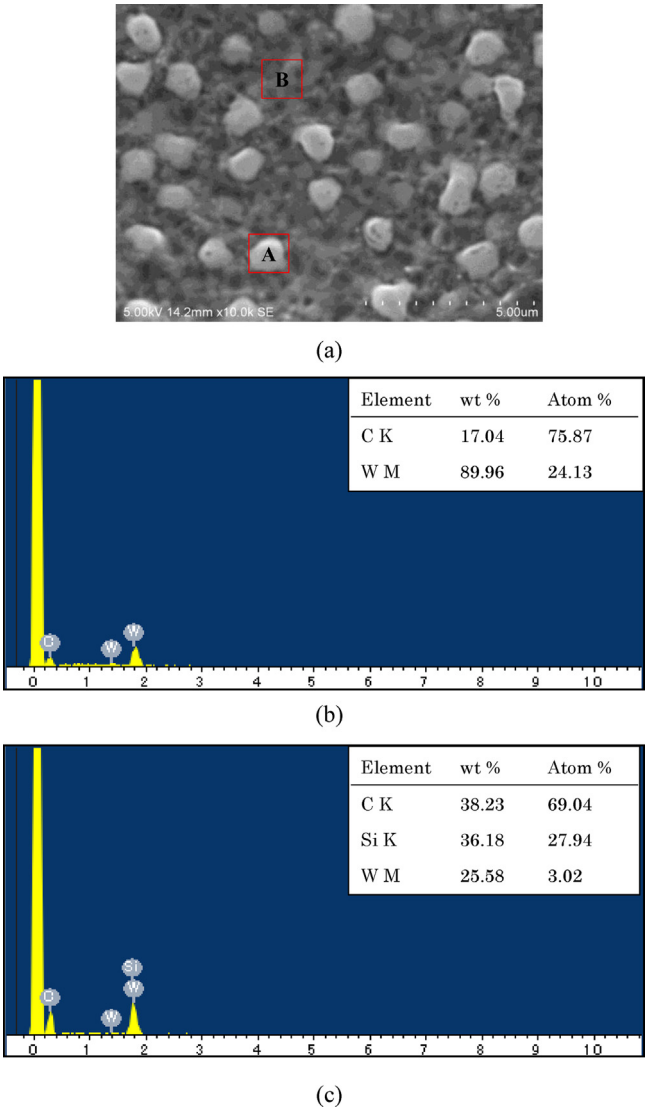

Fig. 5. (a) SEM micrograph of the location mapped by EDX (b) EDX spectrum analysis at zone A (c) EDX spectrum analysis at zone B.

3.2. Effect of voltage

Figs. 6 and 7 present SEM micrographs of machined RB-SiC surfaces at different voltages from 60 V to 110 V under conditions with/without carbon nanofibres addition, respectively. When a low voltage (60 V) was used, the quantity of the deposited tungsten particles is high, as shown in Figs. 6(a) and 7(a). However, as the voltage increases (110 V), the deposited tungsten particles reduce rapidly, as shown in Figs. 6(d) and 7(d). Fig. 8 shows changes in tungsten weight percentage with voltage. It can be seen that for both conditions (with/without carbon nanofibres), the weight percentage of deposited tungsten material decreases significantly as voltage increases.

The effect of voltage on material deposition might be explained from the viewpoint of spark gap between the electrode and workpiece. According to Chung et al. [29], the spark gap is influenced by discharge energy, and the gap increases with the increase of voltage [30]. During fine finishing with low

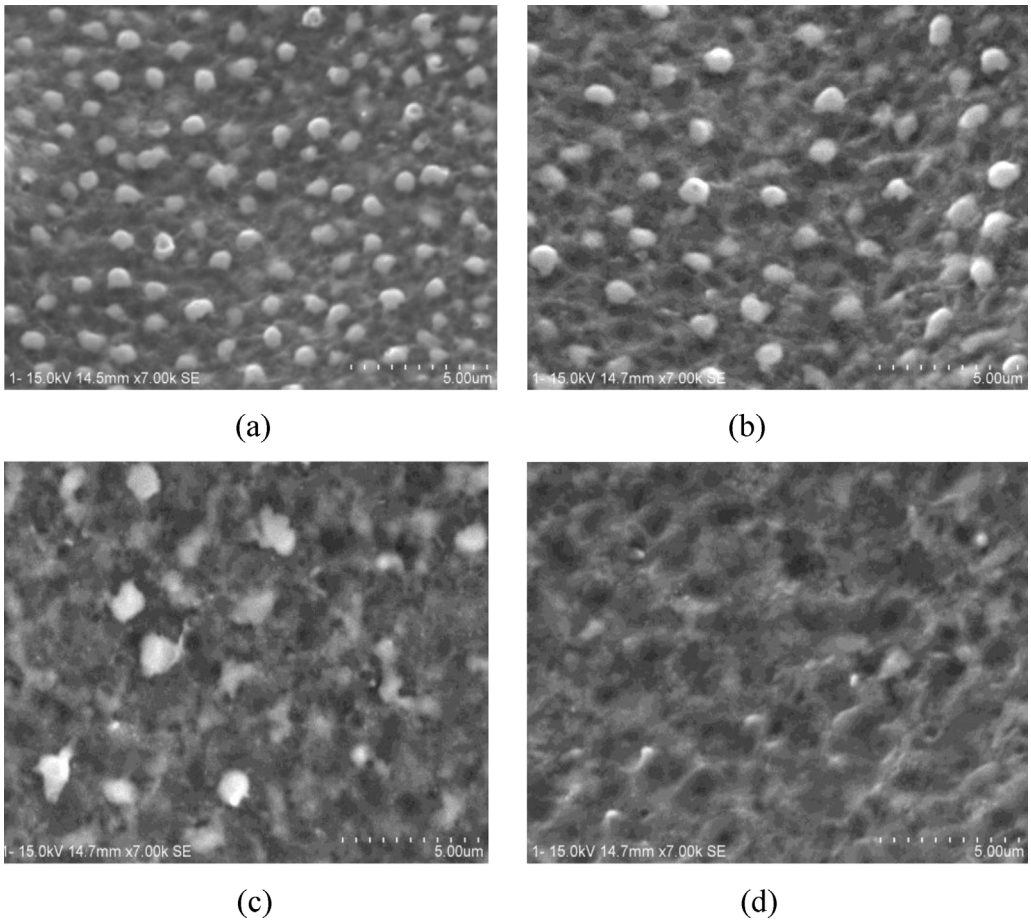

Fig. 6. Machined surface at stray C but different levels of voltage with carbon nanofibres addition: (a) 60 V (b) 80 V (c) 100 V (d) 110 V.

voltage, the gap between the tool and workpiece is very small. Therefore, the electrical discharge-induced tungsten debris cannot be removed effectively from the gap, and instead, be deposited on the machined surface. However, when the voltage increases, the spark gap becomes larger. This makes flushing of tungsten debris easier, resulting in a decrease in material deposition.

In Fig. 8, it is worth noting that by using carbon nanofibre additive, tungsten material deposition becomes lower than that obtained with pure dielectric fluid. When carbon nanofibres are added into the dielectric fluid, the insulating strength of dielectric fluid will be reduced, causing a bigger discharge gap between the tool electrode and the workpiece [25]. Thus, tungsten debris will be flushed out effectively from the gap and deposition will be prevented. This result strongly demonstrates that adding carbon nanofibres in the dielectric fluid is helpful for preventing electrode material deposition on the machined surface.

3.3. Effect of capacitance

Next, the effect of capacitance on deposition of tungsten tool material on machined surface was investigated. Figs. 9 and 10 show SEM micrographs of the machined surface by micro EDM obtained with/without carbon nanofibres addition, respectively. The capacitance ranged from stray capacitance (~1 pF) to 3300 pF at a constant voltage of 60 V. It is seen that the size of the deposited particles increases when higher capacitance is used. A few deposited tungsten particles tend to combine to each other in the capacitance range from 110 pF to 3300 pF.

The size of the deposited tungsten particles was then measured by Talymap software. An example of particle size measurement is shown in Fig. 11. Fig. 12 shows the change in size of the deposited tungsten particles with capacitance. It is seen that the particle size increases with the capacitance for both conditions with/without carbon nanofibres. This is consistent with the change in tungsten weight percentage analyzed by EDX, as shown in Fig. 13. It is known that capacitance had less effect on the machining gap than the voltage did [29]. However, the higher the capacitance is, the longer the discharge duration is [9]. Therefore, the amount of migration and deposition of tool material will be higher when longer discharge duration is used, provided that the machining gap is constant.

Nevertheless, beyond 110 pF, when carbon nanofibers were added, the tungsten debris deposition rate and particle size were higher than that obtained with pure dielectric fluid. At high capacitance, the highly conductive CNFs activated the discharging effect and caused the tool wear rate to increase. Hence, the possibility for tungsten debris to be deposited on the workpiece surface will be higher. Furthermore, with the addition of carbon nanofibres in dielectric oil, discharge-induced craters become shallow and flat, which makes the tungsten particles easy to combine to each other, forming bigger size of tungsten particles. In contrast, the particle size and deposition rate

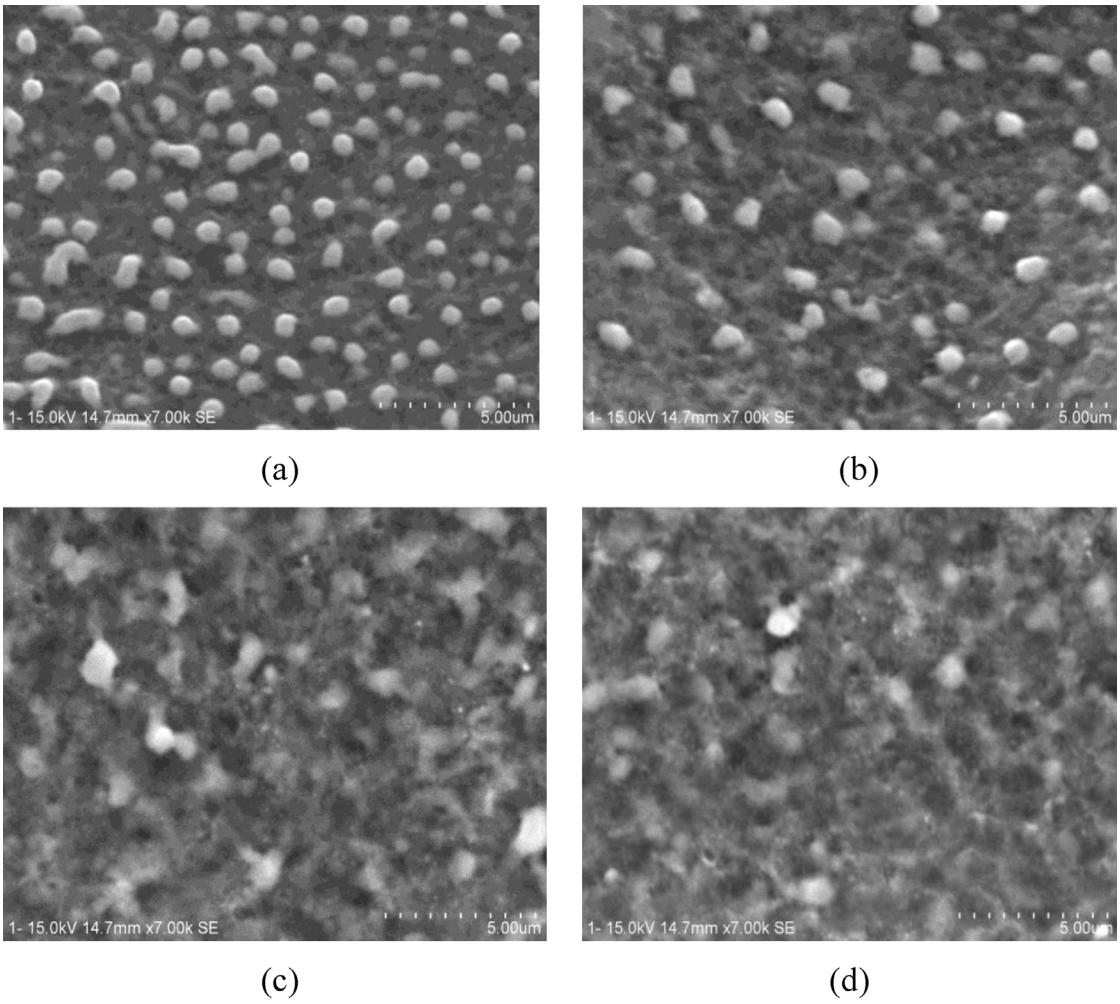

Fig. 7. Machined surface at stray C but different levels of voltage without carbon nanofibres addition: (a) 60 V (b) 80 V (c) 100 V (d) 110 V.

were lower with the use of carbon nanofibres below 10 pF. This indicates that there might be a range of capacitance between 10 pF and 110 pF where the use of carbon nanofibres and pure dielectric oil make no difference on the size of particle and deposition rate. Unfortunately, the verification of this issue was not currently supported by the present experimental setup of the authors.

3.4. *Effect of carbon nanofibre concentration*

Fig. 14 illustrates the effect of carbon nanofibre concentration on the weight percentage of deposited tungsten material. The weight percentage of deposited tungsten material decreases with the carbon nanofibre concentration until 0.06 g/L. As the concentration increases further, the material deposition tends to increase. As carbon nanofibre concentration increases beyond 0.20 g/L, material deposition decreases again. It is noteworthy that the trend of material deposition in Fig. 14 is very similar to that of the surface roughness as we demonstrated in our previous paper [25]. This fact indicates that tool material deposition is affected by surface roughness. As the tungsten debris is easy to be deposited in the craters on the machined surface, the smaller the crater size is (the lower the surface roughness is), the lower the material deposition is [31]. From this meaning, it is presumable that by using a suitable amount of carbon nanofibres, surface roughness will be improved and tungsten material deposition could be prevented. In the present study, the optimum concentration is 0.06 g of CNFs per litre capacity of the dielectric fluid (EDM oil CASTY-LUBE EDS).

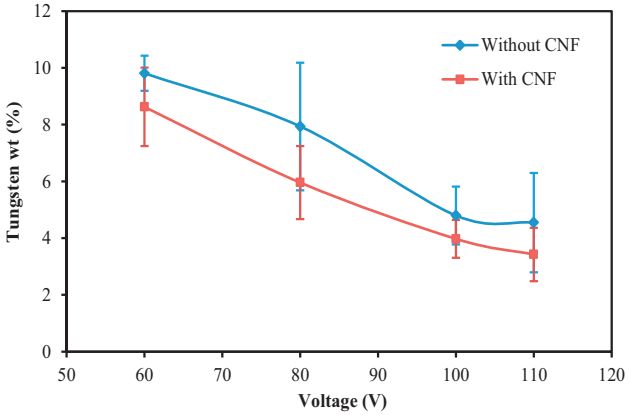

Fig. 8. Effect of voltage on weight percentage of deposited tungsten electrode material.

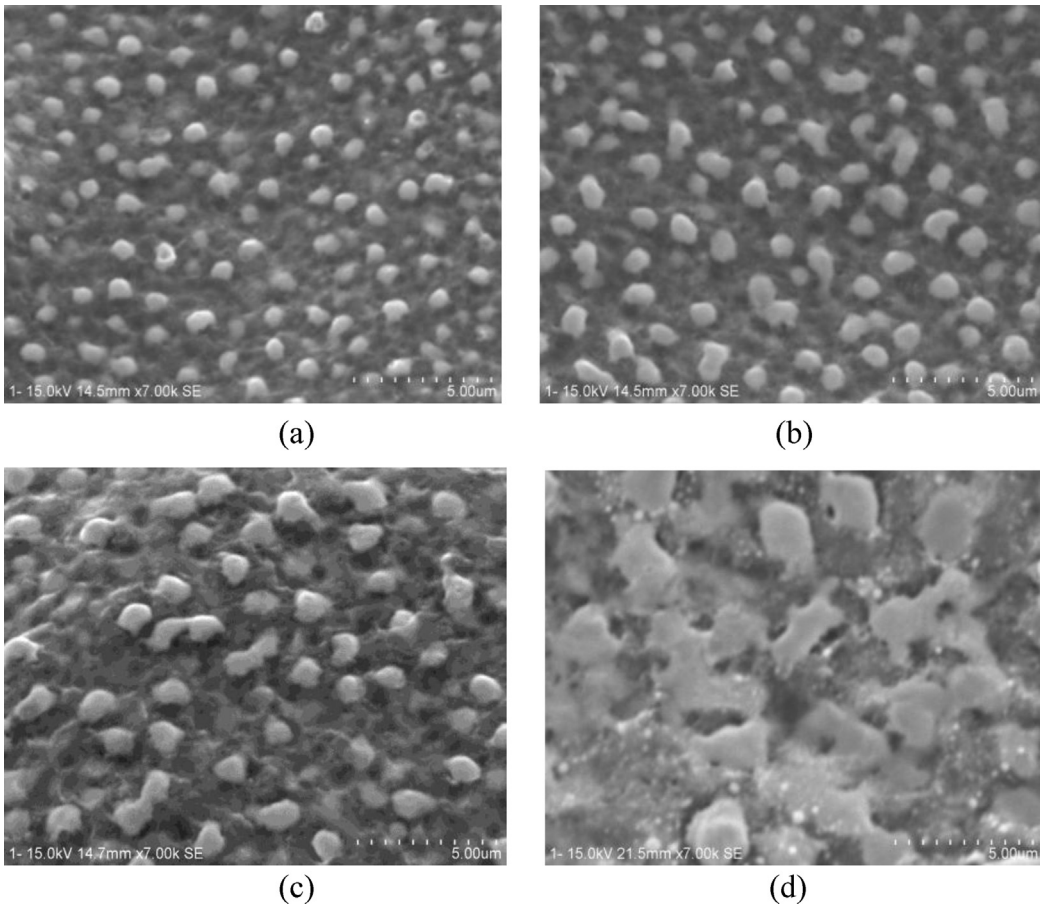

Fig. 9. Machined surface at the same voltage 60 V but different levels of capacitance with carbon nanofibres addition: (a) stray C (b) 10 pF (c) 110 pF (d) 3300 pF.

3.5. Cross-sectional TEM observation

To examine the microstructures of the deposited material, the machined surface was cross-sectioned by mechanical polishing and FIB, and observed by SEM and TEM, respectively. Fig. 15 shows SEM micrograph of machined surface after polishing of the cross section. It is seen that white tungsten particles with an average size around 1 μm were deposited inside the craters on the machined surface. A few tungsten particles might have been removed partially from the surface during polishing, leaving residual white layers.

Fig. 16 is a cross-sectional TEM micrograph of a micro cavity machined at 70 V and stray capacitance (∼1 pF). It is seen that tungsten particles (black region A) were firmly deposited in the crater of the workpiece which is composed of 6H-SiC and Si grains. On the surface where W particles were not deposited, a dark layer of material (region B) with a thickness of approximately 40–50 nm is formed, the compositions and microstructure of which looks different from the bulk material. To confirm the microstructure of the deposited particle and dark layer, electron diffraction analysis was done using the TEM, as shown in Fig. 17. In Fig. 17(a), only fuzzy rings are shown, indicating that the deposited tungsten in Zone A has an amorphous structure. In contrast, in Fig. 17(b), a series of concentric rings resulting from many diffraction spots also can be seen, demonstrating that the deposited dark layer on the machined surface is poly-crystalline.

Similar amorphous/poly-crystalline layers on bulk materials have also been observed in mechanical machining processes. For example, in the diamond turning of RB-SiC [32], amorphization of silicon matrix and dislodgement of SiC grains were confirmed. In diamond cutting of single crystalline silicon [33], an amorphous layer with a thickness ranging from the nanometre level to the submicron level was formed on the workpiece surface. In single point diamond turning of single-crystal SiC (6H) [34], original single-crystal SiC material was transformed into an amorphous material, on the surface and within the chip. Subsurface deformation of various types of single crystal SiC was also confirmed in molecular dynamics simulation of nanometre level cutting [35], and the subsurface crystal lattice deformed layer depths were quantified by subtracting the uncut chip thickness. However, it should be noted that in this study, the amorphous/poly-crystalline layer is deposited on the workpiece from the tool electrode and not phase-transformed from the bulk material by mechanical stresses. From this meaning, we can say that the formation mechanism of the subsurface layer in this work is distinctly different from those in mechanical machining processes such as diamond turning.

To further confirm the elemental composition of the deposited material in zone A and zone B, EDX analysis was done on the cross section of the sample, as depicted in Fig. 18. Fig. 18(a) clearly shows that the deposited material in zone A is tungsten (W). However, in

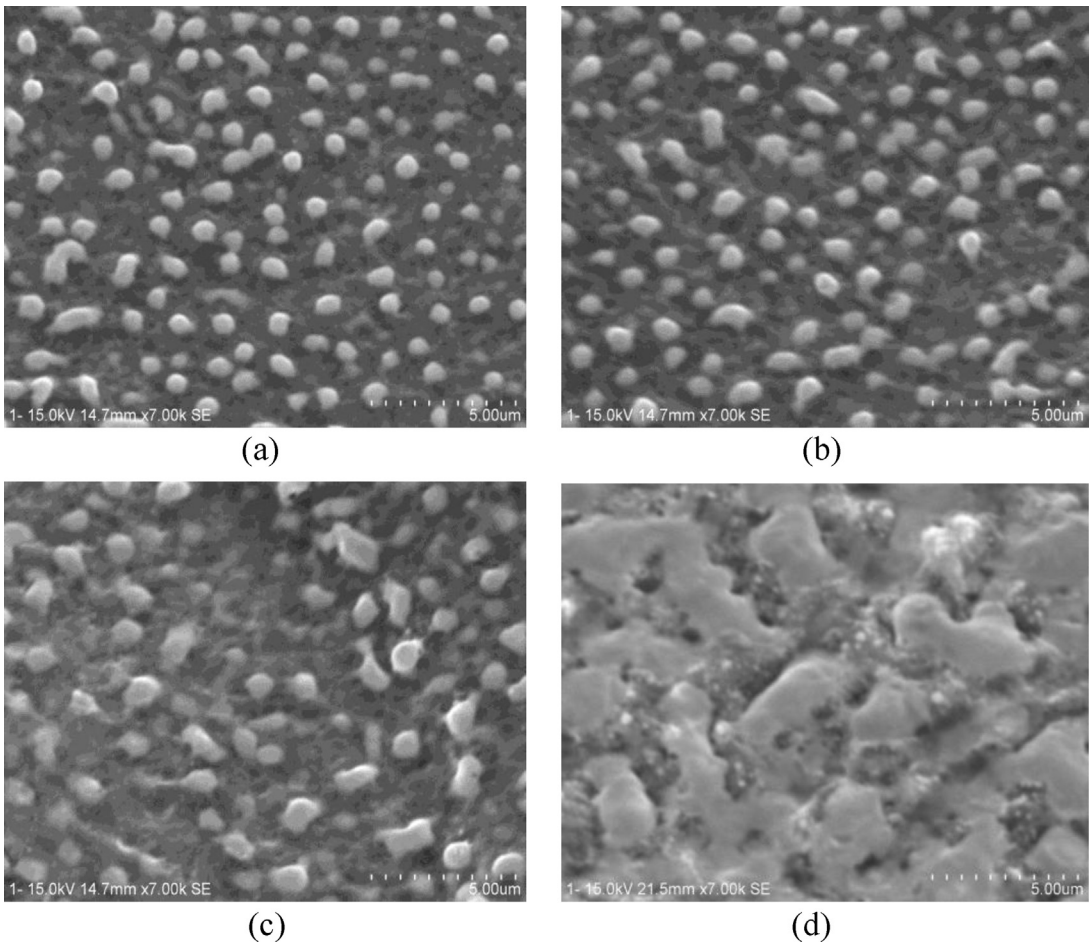

Fig. 10. Machined surface at the same voltage 60 V but different levels of capacitance without carbon nanofibres addition: (a) stray C (b) 10 pF (c) 110 pF (d) 3300 pF.

Fig. 18(b), besides tungsten (W), carbon (C) and silicon (Si) were also found, indicating that the interdiffusion of tungsten, silicon and carbon might have occurred. These cross- sectional EDX results agree well with the surface EDX results in Fig. 5.

The cross-sectional sample of the tungsten electrode tip after the EDM process was also examined using TEM. In Fig. 19, micro craters were found on the tungsten electrode tip, verifying that some of the tungsten grains were melted and removed during the EDM process. The EDX analysis results in Fig. 20(a) indicated that carbon (C) exists on the tungsten electrode tip, whereas no C element was detected inside the tool material (Fig. 20b). The C element on the electrode surface might have been migrated from either the workpiece material or the CNFs. Another explanation is that the C element might be generated during the decomposition of dielectric oil at high temperature in EDM.

3.6. Material migration mechanism

A schematic model for material migration is shown in Fig. 21. During the EDM process, the Si matrix, in conjunction with sintering agents, possesses a higher electrical conductivity than the 6H-SiC grains, so it is preferentially removed by melting and vaporization [1], leaving craters on the surface (Fig. 21(a)). At the same time, heat concentration on the electrode causes the electrode surface melted. The melted electrode material maybe migrated towards the workpiece under an electric field, then resolidified and deposited onto the workpiece. The melted tungsten is easier to be deposited inside the craters than the flat regions, forming small particles, as depicted in Fig. 21(b). Similarly, Murray et al. [36] reported that nm-sized tungsten crystals from electrode were mixed in with the discharge melt pool, as solid particles and their crystalline structure is maintained. In the flat region, however, a thin interdiffusion layer is generated where the melted tungsten reacted with silicon and carbon from the workpiece material. According to Mohri et al. [37], the deposition of electrode material changed the characteristics of the workpiece surface. After EDM, the workpiece surface has fewer cracks, higher corrosion resistance and wear resistance. On the other hand, tool material deposition will cause surface contamination and surface roughening of the workpiece. Therefore, generally speaking, material migration should be promoted in rough machining and suppressed in fine machining.

Based on the experimental results obtained in this study, we may say that for reducing the migration and deposition of tool material, the capacitance should be kept as low as possible and the voltage at moderately high level. Adding carbon nanofibres into the dielectric fluid at a concentration of 0.06 g/l capacity of dielectric fluid is helpful. These findings are useful for improving the surface integrity and purity of RB-SiC in micro EDM.

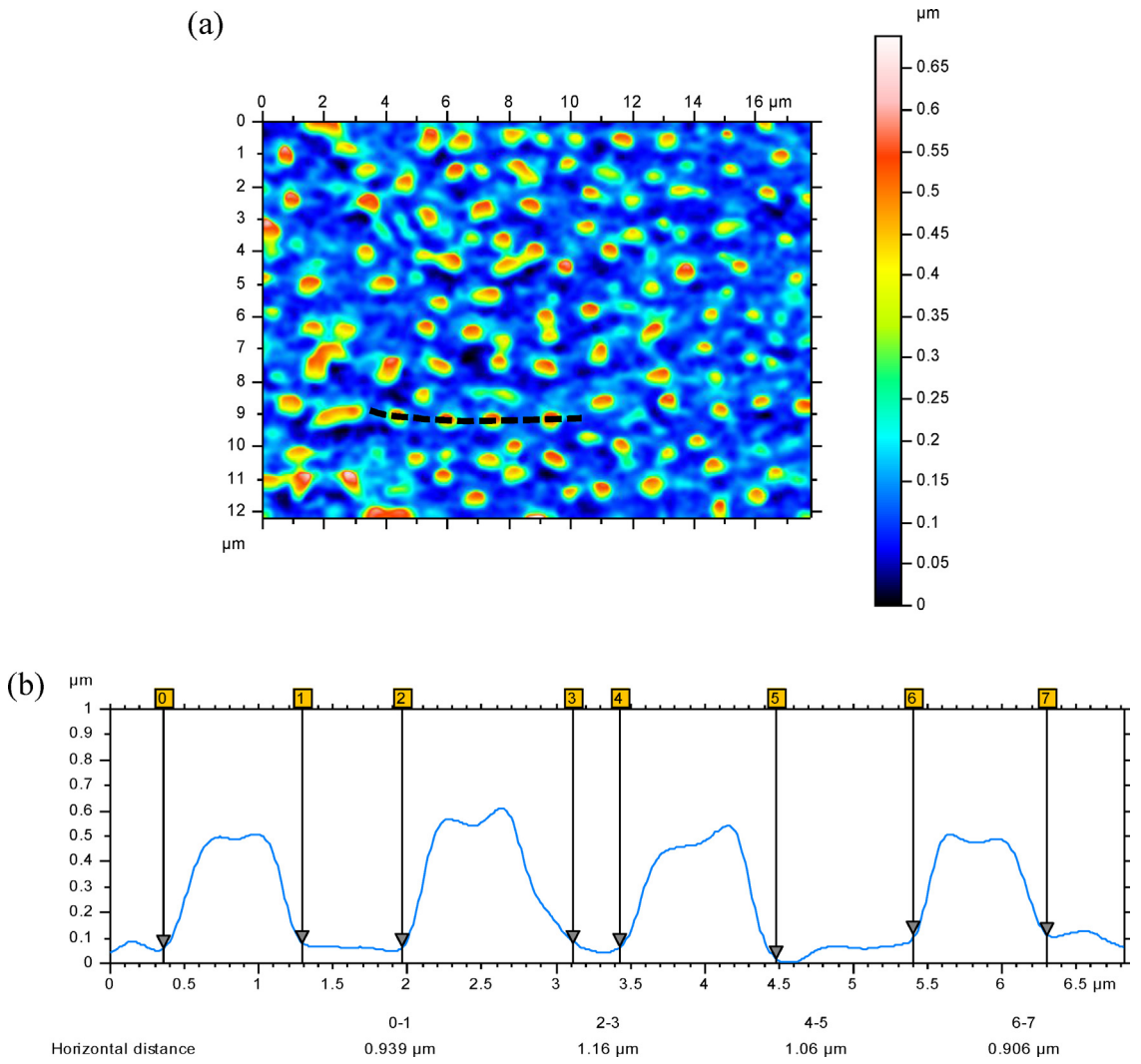

Fig. 11. (a) Mapping image of machined surface with deposited tungsten tool particles and (b) measurement of the particle size by extracting the cross sectional profile.

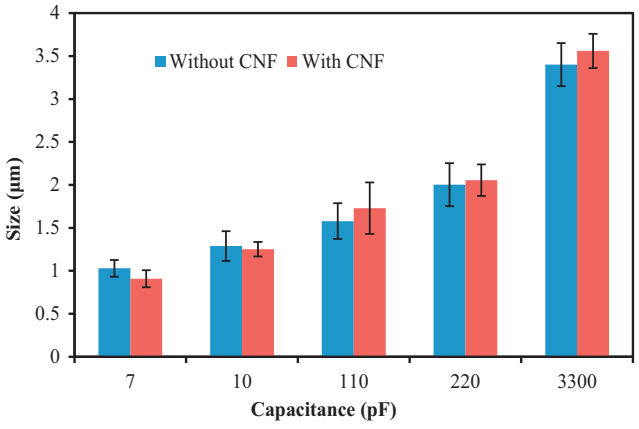

Fig. 12. Effect of capacitance on the size of deposited tungsten particles.

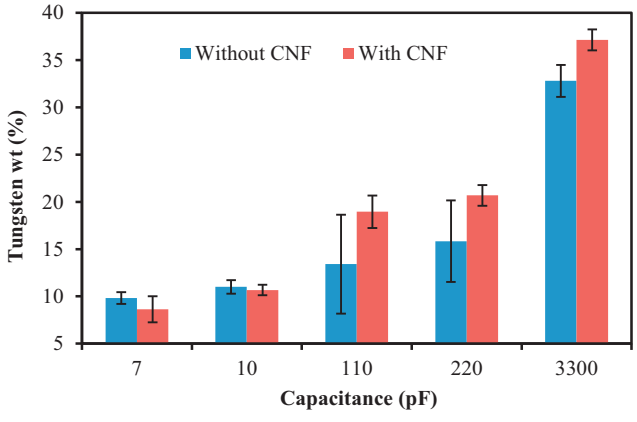

Fig. 13. Effect of capacitance on the weight percentage of deposited tungsten particles.

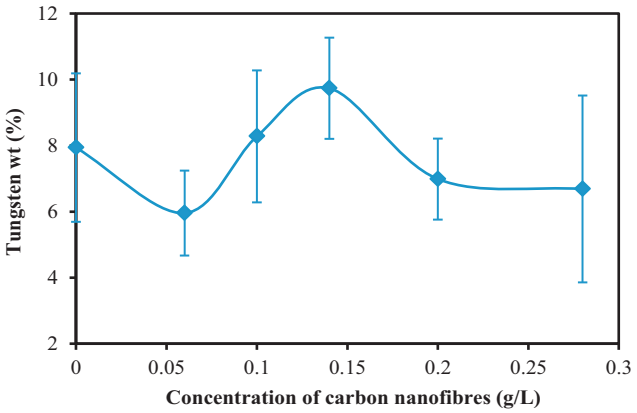

Fig. 14. Effect of carbon nanofibres concentration on weight percentage of deposited tungsten tool material.

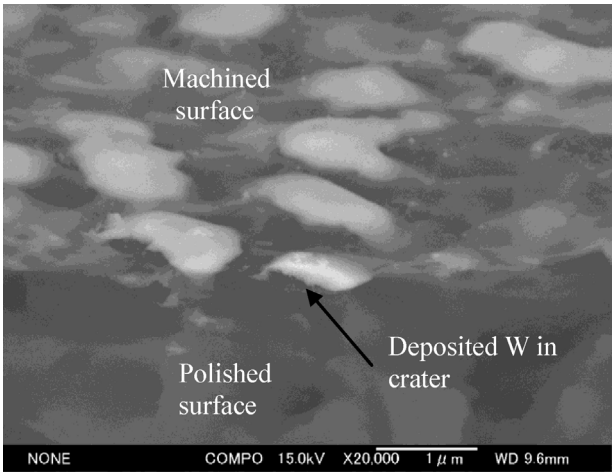

Fig. 15. SEM micrographs of machined surface after surface polishing.

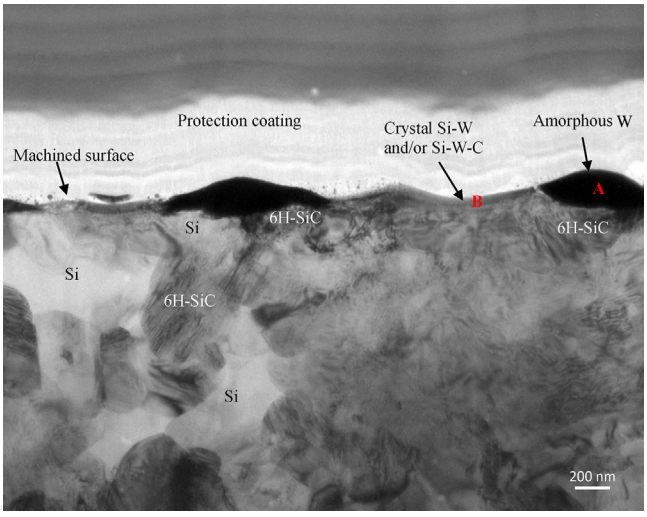

Fig. 16. Cross-sectional TEM micrograph of micro cavity machined at 70 V and stray capacitance.

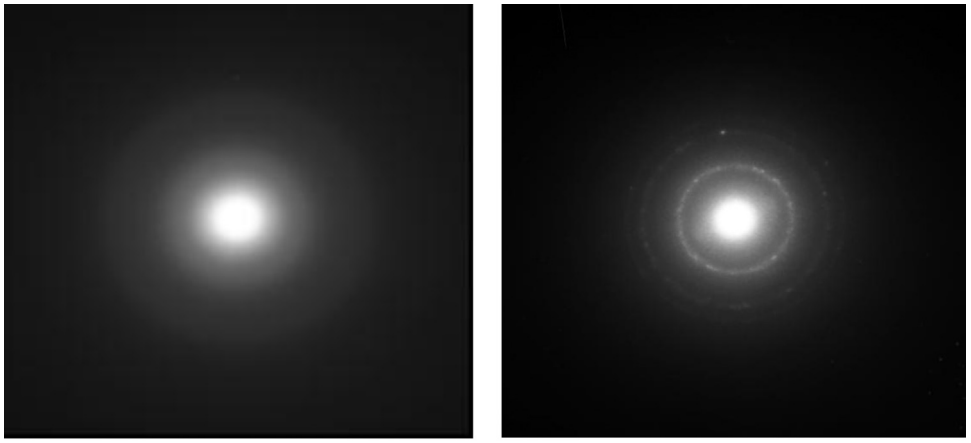

Fig. 17. Electron diffraction pattern at: (a) zone A, indicating an amorphous structure and (b) zone B, showing a crystalline structure.

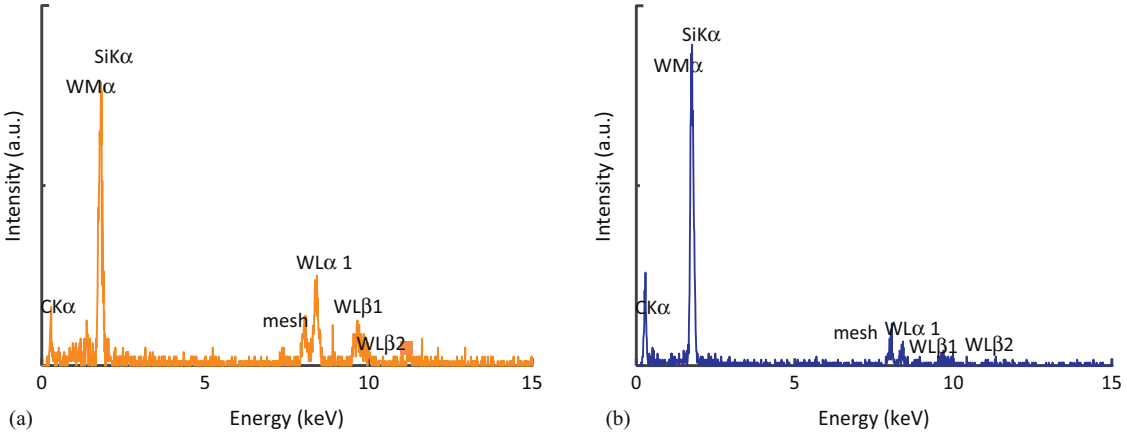

Fig. 18. EDX spectrum analysis at: (a) zone A and (b) zone B in Fig. 16.

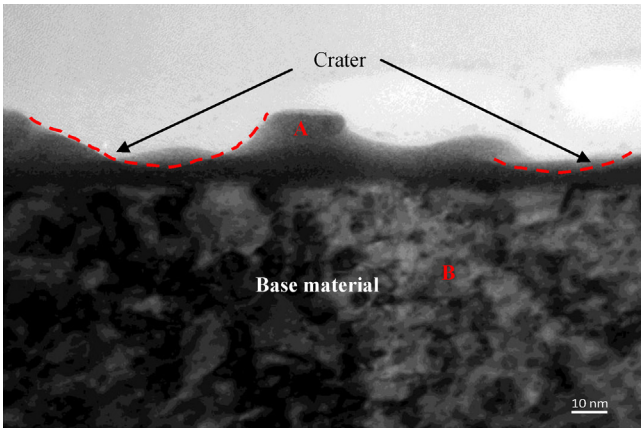

Fig. 19. Cross-sectional TEM micrograph of tungsten electrode tip after EDM process.

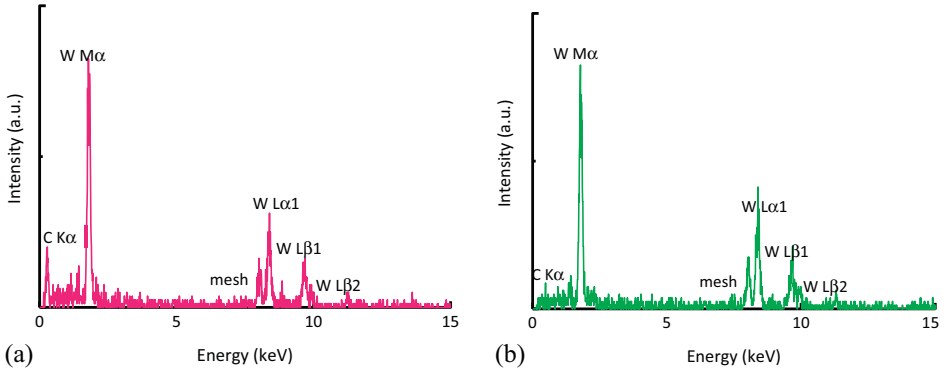

Fig. 20. EDX spectrum analysis at: (a) zone A and (b) zone B in Fig. 19.

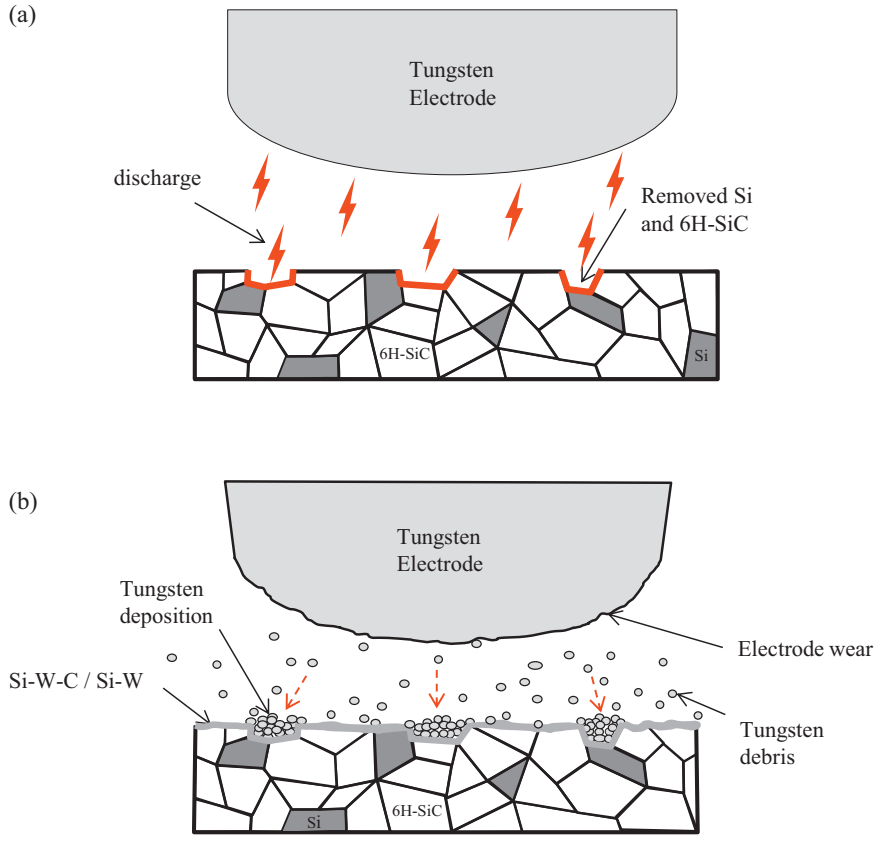

Fig. 21. Schematic models for (a) material removal of Si and 6H-SiC during micro EDM and (b) deposition of electrode material on workpiece surface.

4. Conclusions

Material migration phenomenon between tool electrode and workpiece material in micro EDM of RB-SiC has been experimentally investigated. The following conclusions were drawn:

(1) Tungsten electrode material is deposited as micro particles in amorphous structure inside surface craters, and as a thin interdiffusion layer of poly-crystalline structure on flat surface regions.
(2) Deposition of carbon element on tool electrode occurs due to material migration from workpiece material, decomposed dielectric oil, or carbon nanofibres in the dielectric.
(3) Material deposition rate is closely related to workpiece surface roughness. The higher the roughness, the higher the deposition rate.
(4) Voltage strongly effects the deposition of tungsten tool material on the workpiece. The lower the voltage is, the more significant the deposition rate is.
(5) Tool material deposition on workpiece material in terms of particle size and weight percentage increases with the capacitance of the electrical discharge circuit.
(6) Carbon nanofibre addition can significantly reduce the deposition of tool material on the workpiece surface. The lowest deposition rate was achieved at a concentration of 0.06 g of CNFs per litre capacity of dielectric fluids.

Acknowledgments

The authors would like to thank Professor Toyohiko Konno of Institute for Materials Research, Tohoku University for his valuable comments and advices. Assistance in TEM sample preparation from Dr. Takamichi Miyazaki and Dr. Yumiko Kodama of School of Engineering, Tohoku Unversity are gratefully acknowledged.

References

[1] W. Konig, D.F. Dauw, G. Levy, U. Panten, EDM-future steps towards the machining of ceramics, Annals of the CIRP 37 (2) (1988) 623–631.
[2] D. Reynaerts, W. Meeusen, H.V. Brussel, Machining of three-dimensional microstructures in silicon by electro-discharge machining, Sensors and Actuators A 67 (1998) 159–165.
[3] N. Mohri, Y. Fukuzawa, T. Tani, N. Saito, K. Furutani, Assisting electrode method for machining insulating ceramics, Annals of the CIRP 45 (1) (1996) 201–204.
[4] Y. Liu, R. Ji, Q. Li, L. Yu, X. Li, Electric discharge milling of silicon carbide ceramic with high electrical resistivity, International Journal of Machine Tools and Manufacture 48 (2008) 1504–1508.
[5] Y.J. Lin, Y.C. Lin, A.C. Wang, D.A. Wang, H.M. Chow, Machining characteristics of EDM for non-conductive ceramics using adherent copper foils, Advanced Materials Research 154–155 (2011) 794–805.
[6] Y. Fukuzawa, N. Mohri, H. Gotoh, T. Tani, Three-dimensional machining of insulating ceramics materials with electrical discharge machining, Transaction of Nonferrous Metals Society of China 19 (2009) 150–156.
[7] S. Clijsters, K. Liu, D. Reynaerts, B. Lauwers, EDM technology and strategy development for the manufacturing of complex parts in SiSiC, Journal of Materials Processing Technology 210 (2010) 631–641.
[8] I. Puertas, C.J. Luis, A study on the electrical discharge machining of conductive ceramics, Journal of Materials Processing Technology 153–154 (2004) 1033–1038.
[9] G. Karthikeyan, A.K. Garg, J. Ramkumar, S. Dhamodaran, A microscopic investigation of machining behavior in μED-milling process, Journal of Manufacturing Processes 14 (2012) 297–306.
[10] J.E. Greene, J.L. Guerrero-Alvarez, Electro-erosion of metal surfaces, Metallurgical Transactions 5 (1974) 695–706.
[11] M.L. Jeswani, S. Basu, Electron microprobe study of deposition and diffusion of tool material in electrical discharge machining, International Journal of Production Research 17 (1) (1979) 1–14.
[12] J.S. Soni, G. Chakraverti, Experimental investigation on migration of material during EDM of die steel (T215 Cr12), Journal of Materials Processing Technology 56 (1996) 439–451.
[13] S. Kumar, U. Batra, Surface modification of die steel materials by EDM method using tungsten powder-mixed dielectric, Journal of Manufacturing Processes 14 (1) (2012) 35–40.

[14] P. Janmanee, A. Muttamara, Surface modification of tungsten carbide by electrical discharge coating (EDC) using a titanium powder suspension, Applied Surface Science 258 (2012) 7255–7265.
[15] A. Gangadhar, M.S. Shunmugam, P.K. Philip, Surface modification in electrodischarge processing with a powder compact tool electrode, Wear 143 (1991) 45–55.
[16] Y.F. Chen, H.M. Chow, Y.C. Lin, C.T. Lin, Surface modification using semi-sintered electrodes on electrical discharge machining, International Journal of Advanced Manufacturing Technology 36 (2008) 490–500.
[17] Y.L. Hwang, C.L. Kuo, S.F. Hwang, The coating of TiC layer on the surface of nickel by electric discharge coating (EDC) with multi-layer electrode, Journal of Materials Processing Technology 210 (2010) 642–652.
[18] J. Simao, H.G. Lee, D.K. Aspinwall, R.C. Dewes, E.M. Aspinwall, Workpiece surface modification using electrical discharge machining, International Journal of Machine Tools and Manufacture 43 (2003) 121–128.
[19] J. Murray, D. Zdebski, A.T. Clare, Workpiece debris deposition on tool electrodes and secondary discharge phenomena in micro-EDM, Journal of Materials Processing Technology 212 (2012) 1537–1547.
[20] J. Mafarona, Black layer characteristic and electrode wear ratio in electrical discharge machining (EDM), Journal of Materials Processing Technology 184 (2007) 27–31.
[21] M.P. Jahan, M. Rahman, Y.S. Wong, Migration of materials during finishing micro-EDM of tungsten carbide, Key Engineering Materials 443 (2010) 681–686.
[22] J.P. Kruth, L. Stevens, L. Froyen, B. Lauwers, Study of the white layer of a surface machined by die-sinking electro-discharge machining, Annals of the CIRP 44 (1995) 169–172.
[23] B. Ekmekci, Residual stresses and white layer in electric discharge machining (EDM), Applied Surface Science 253 (2007) 9234–9240.
[24] P.F. Thomson, Surface damage in electrodischarge machining, Material Science Technology 5 (1989) 1153–1157.
[25] P.J. Liew, J. Yan, T. Kuriyagawa, Carbon nanofibre assisted micro electro discharge machining of reaction-bonded silicon carbide, Journal of Materials Processing Technology 213 (7) (2013) 1076–1087.
[26] Technical data provided by the manufacturer of the workpiece material.
[27] Technical data provided by the manufacture of the tungsten rod, available from http://www.nittan.co.jp/en/index.html
[28] http://taylor-hobson.virtualsite.co.uk/optics_talymap3d.htm
[29] D.K. Chung, B.H. Kim, C.N. Chu, Micro electrical discharge milling using deionized water as a dielectric fluid, Journal of Micromechanics and Microengineering 17 (2007) 867–874.
[30] F.L. Amorim, W.L. Weingaertner, The influence of generator actuation mode and process parameters on the performance of finish EDM of a tool steel, Journal of Materials Processing Technology 166 (2005) 411–416.
[31] M.B. Ranade, Adhesion and removal of fine particles on surfaces adhesion, Aerosol Science and Technology 7 (2) (1987) 161–176.
[32] J. Yan, Z. Zhang, T. Kuriyagawa, Mechanism for material removal in diamond turning of reaction-bonded silicon carbide, International Journal of Machine Tools and Manufacture 49 (5) (2009) 366–374.
[33] J. Yan, T. Asami, H. Harada, T. Kuriyagawa, Fundamental investigation of subsurface damage in single crystalline silicon caused by diamond machining, Precision Engineering 33 (4) (2009) 378–386.
[34] J. Patten, W. Gao, K. Yasuto, Ductile regime nanomachining of single-crystal silicon carbide, ASME Journal of Manufacturing Science and Engineering 127 (2005) 522–532.
[35] X. Luo, S. Goel, R.L. Reuben, A quantitative assessment of nanometric machinability of major polytypes of single crystal silicon carbide, Journal of the European Ceramic Society 32 (2012) 3423–3434.
[36] J.W. Murray, M.W. Fay, M. Kunieda, A.T. Clare, TEM study on the electrical discharge machined surface of single-crystal silicon, Journal of Materials Processing Technology 213 (2013) 801–809.
[37] N. Mohri, N. Saito, Y. Tsunekawa, Metal surface modification by electrical discharge machining with composite electrodes, Annals of the CIRP 42 (1) (1993) 219–222.